DATE: 09.27.95

ARESE (ARM Enhanced Shortwave Experiment)

SCIENCE PLAN

Francisco P. J. Valero, Stephen E. Schwartz, Robert D. Cess, V. Ramanathan, William D. Collins, Patrick Minnis, Thomas P. Ackerman, John Vitko, and Tim P. Tooman

DISCLAIMER

DISCLAIMER

Portions of this document may be illegible in electronic image products. Images are produced from the best available original document.

SUMMARY

Several recent studies have indicated that cloudy atmospheres may absorb significantly more solar radiation than currently predicted by models. The magnitude of this 'excess atmospheric absorption', is about 50% more than currently predicted and would have major impact on our understanding of atmospheric heating. Incorporation of this 'excess heating' into existing general circulation models also appears to ameliorate some significant shortcomings of these models, most notably a tendency to overpredict the amount of radiant energy going into the oceans and to underpredict the tropopause temperature. However, some earlier studies do not show this 'excess absorption' and an underlying physical mechanism that would give rise to such absorption has yet to be defined. Given the importance of this issue, the Department of Energy's (DOE) Atmospheric Radiation Measurement (ARM) program is sponsoring the ARM Enhanced Shortwave Experiment (ARESE) to study the absorption of solar radiation by clear and cloudy atmospheres.The experimental results will be compared with model calculations. Measurements will be conducted using three aircraft platforms (ARM-UAV Egrett, NASA ER-2, and an instrumented Twin Otter), as well as satellites and the ARM central and extended facilities in North Central Oklahoma. The project will occur over a four week period beginning in late September, 1995. Spectral broadband, partial bandpass, and narrow bandpass (10nm) solar radiative fluxes will be measured at different altitudes and at the surface with the objective to determine directly the magnitude and spectral characteristics of the absorption of shortwave radiation by the atmosphere (clear and cloudy). Narrow spectral channels selected to coincide with absorption by liquid water and ice will help in identifying the process of absorption of radiation. Additionally, information such as water vapor profiles, aerosol optical depths, cloud structure and ozone profiles, needed to use as input in radiative transfer calculations, will be acquired using the aircraft and surface facilities available to ARESE. This document outlines the scientific approach and measurement requirements of the project.

SUMMARY

Recent field measurements have brought into question the present understanding of shortwave absorption by clouds and suggested that clouds absorb shortwave radiation in amounts which would be of great significance in atmospheric models and which are not now represented in these models. These studies indicate the need for further examination of the absorption of solar radiation by the atmosphere both theoretically and experimentally, because of the major potential consequences associated with the uncertainties in present day understanding of atmosphere-clouds-radiation interactions. The ARM Enhanced Shortwave Experiment (ARESE) will be conducted to study the absorption of solar radiation by the clear and cloudy atmosphere. The experimental results will be compared with model calculations. Measurements will be conducted using three aircraft platforms (DOE high altitude testbed unmanned aerospace vehicle, NASA ER-2, and an instrumented Twin Otter), as well as satellites and the ARM central and extended facilities in North Central Oklahoma. The project will occur over a four week period beginning in late September, 1995. Spectral broadband, partial bandpass, and narrow bandpass (10 nm) solar radiative fluxes will be measured at different altitudes and at the surface with the objective to determine directly the magnitude and spectral characteristics of the absorption of shortwave radiation by the atmosphere (clear and cloudy). Narrow spectral channels selected to coincide with absorption by liquid water and ice will help in identifying the process of absorption of radiation. Additionally, information such as water vapor profiles, aerosol optical depths, cloud structure and ozone profiles, needed to use as input in radiative transfer calculations, will be acquired using the aircraft and surface facilities available to ARESE. This document outlines the scientific approach and measurement requirements of the project.

Flight track B is a triangle with vertices at the Lamont central facility, and at the Ringwood and Byron extended facilities. The flight path lengths are (beginning with Lamont, heading toward Ringwood, and including the dogleg) 75 km, 50 km, and 78 km respectively.

Flight track C is near linear between the Lamont and Coldwater extended facilities, overflying the Byron site along the way. The flight path including a slight bend is 182 km long in the WNW- ESE direction.

Flight track D is also near linear between the Lamont and Vici extended facilities, overflying the Ringwood site along the way. The flight path including two slight bends is 163 km long in the WSW - ENE direction.

As mentioned above the ER-2 will follow the same tracks at its operational altitude.

FORECASTING

As in all field experiments that utilize research aircraft, accurate meteorological forecasting will prove to be an important component of the experiment operation. Based on our previous experience in forecasting for aircraft-based field programs, one of the essential requirements is immediate access to the most recent satellite imagery. While satellite imagery via the Internet is available, the delay between image acquisition and its posting on the Internet tends to be on the order of 1-2 hours. This delay time proved to be a significant hindrance during the field deployment at the CART site during April 1994. To solve this problem, a McIdas would be required. On the McIdas system, imagery is available in near-real time and image enhancement and image animation significantly aids in accurate forecasting. In addition to the McIdas system, Internet access is important for acquiring model output and additional information necessary for preparing daily briefings. The forecasting team should be composed of at least two experienced meteorologists (?).

SATELLITE ISSUES FOR ARESE

Cloud forcing at the top of the atmosphere has generally been measured using satellites such as the ERBS or GOES. The satellites provide global coverage and have been used to determine the spatial variability of cloud radiative forcing at scales ranging from 8 to 250 km. A considerable portion of the evidence pointing to increased SW absorption in cloudy skies has been derived from combined surface and satellite datasets. Past studies have shown a consistency between aircraft and satellite-derived, cloudy-sky SW absorption. However, the satellite and aircraft experiments were carried out at different times and places. ARESE will provide the opportunity to have coincident satellite and aircraft measurements over extended time periods. Independent analyses using various combinations of aircraft, surface, and satellite data will provide a more comprehensive assessment of the apparent anomalous absorption phenomenon than has been previously possible.

The only useful satellite data for the ARESE time period will be from the narrowband visible (VIS) channels on the meteorological satellites GOES, NOAA, and Meteosat (if it is still operating in the U.S. domain). These satellites use scanning radiometers that measure radiances in the visible (0.55 - 0.75 μm), mid near-infrared (0.85 - 1.6 μm), near-infrared (3.6 - 4.0 μm), and infrared window (10 -12.8 μm) spectral regions. Broadband scanners such as those on the ERBS, SCARAB, and TRMM (CERES) spacecraft will not be available during the ARESE time frame. Thus, all of the satellite measurements of SWCRF must be based on SW fluxes inferred from the VIS radiances on the meteorological satellites. The fluxes derived from the satellites are sensitive to the narrowband calibrations, the narrowband-to-broadband conversions, and the anisotropic reflectance properties of a given scene.

Most of the operational meteorological satellites have provisions for maintaining stable in-flight calibrations for their thermal channels. The calibrations of their visible and near-infrared sensors are not so well supported, relying on relatively infrequent, dedicated flights of the NASA ER-2. Calibration of the narrowband VIS channels will be effected using collocated and co-angled satellite VIS and ER-2 MAS 0.63 μm reflectances taken during the ARESE. Initial analyses of the satellite data will use nominal, updated, or AVHRR-normalized calibrations depending on availability. The data will be reanalyzed using the ER-2-based calibrations if necessary.

In the past, either empirical or theoretical techniques were used to convert the narrowband data to broadband fluxes. However, because most of the fluxes are derived from radiance measurements, there are uncertainties due to both spectral and directional effects. These uncertainties must be evaluated in order to draw quantitative conclusions from the analyses.

The satellite portion of ARESE has several components that range from the calibration of the satellite VIS channels to determination of CRF over the surface sites and along the aircraft flight tracks to estimation of the instantaneous and average uncertainties in the derived products. These experiment tasks are detailed below.

1) Calibration of narrowband meteorological satellite sensors

Calibration of the satellite VIS channels requires a well-calibrated set of sensors on the ER-2 or UAV. The MAS and MPIR will be the main sensors for performing the narrowband satellite calibrations. It is expected that their calibrations will be well known during the ARESE flights. The essential elements for this experiment include BBSS (balloon borne sounding system) profiles, a characterization of the stratosphere including aerosol and ozone loading, and MAS and MPIR radiances. A characterization of the underlying bi-directional reflectance field is also desirable.

The calibration experiment should be executed near the central facility using the UAV at maximum altitude and/or the ER-2. The UAV and/or the ER-2 should be flown parallel to the flight path of the Sun-synchronous NOAA satellites and on an azimuth perpendicular to the satellite azimuth for the geostationary satellites. Calibration of the AVHRR channels should be performed for both the morning and afternoon NOAA satellites. Most of the calibration flights for AVHRR should be executed whenever the satellite viewing zenith angle (VZA) is less than 40 deg. Calibrations should be performed for higher VZAs to determine the uncertainty induced by the atmospheric corrections and the angular configurations. For the GOES and Meteosat satellites, the UAV will have to fly in a roll sufficient to extend the maximum MPIR VZA to a few degrees beyond the satellite VZA at the SGP central facility. The current satellite positions yield VZAs of 44, 48, and 54 degrees for GOES-8, Meteosat-4, and GOES-7 (GOES-9 after a summer launch), respectively. All three satellites require a linear flight pattern with a sustained roll of 15 to

20 degrees. These satellite positions are subject to change but the minimum geostationary VZA for the central facility in Oklahoma is ~ 40 deg. These VZAs may limit the ER-2 calibrations to one or two of the considered satellites.

The calibration legs should last for a minimum of 10 minutes. Normally, the satellite view constitutes a snapshot of the scene. Thus, there are only one or two satellite pixels that actually coincide with the MPIR or MAS views. The others must be normalized or renavigated to match the aircraft views. With the potential for rapid rescanning, it may be possible for the GOES-8 to rescan the central facility area every few minutes to maintain coincidence between the satellite and aircraft views. This rescanning mode requires a special request to the GOES operations manager. Because the geostationary satellites generally produce images every hour or half hour, it will be possible to use multiple images to generate additional collocated aircraft-satellite pixels. The MPIR field of view (FOV) yields a pixel resolution of ~ 0.1 km at the surface when the UAV is at an altitude of 15 km.

The nominal pixel size is 1 km for all AVHRR channels and for the GOES VIS channel. However, it is 2.5 km for the Meteosat VIS channel. Matching the MPIR (MAS) and satellite FOVs requires averaging of the MPIR (MAS) pixels both along and across the flight track. However, as the pixels are averaged across track, the VZA changes. A 1-km satellite pixel would need approximately 3-4 deg of VZA from the MPIR at the maximum altitude. Spatial correlations will be used to match the MPIR (MAS) and satellite pixels after initial navigation corrections. Because it will not be possible to match the satellite and averaged MPIR (MAS) pixels exactly, it will be necessary to use additional satellite pixels on either side of the primary FOVs, resulting in a total angular coverage of nearly 10 deg of VZA. The angular and mismatched pixels will introduce errors into the calibration. It is expected that those errors can be diminished by maximizing the sampling. All flights should be carried out over clear conditions and relatively uniform low stratus or large-celled stratocumulus to maximize the dynamic range of the calibration and maintain the greatest separation between the targets and the UAV.

An uplooking CDL on the UAV can be used to profile the stratosphere for aerosol loading. An uplooking TDDR on the UAV (ER-2) would be desirable for estimating the aerosol optical depth above the aircraft. Assuming similar calibrations between the two

instruments, it will be possible to cross-check the MPIR-satellite and MAS-satellite calibrations and to assess the atmospheric corrections to some extent since there will be approximately 6 km between the two aircraft. The BBS should be launched prior to the satellite overpass so that they reach the stratosphere during the overpass. Ozone measurements are also needed for the stratosphere. Bi-directional reflectance characteristics of the surface are needed to assess the diffuse component of the upwelling radiances. Such measurements could be provided a priori from appropriately instrumented helicopter flights.

The calibrations will be effected by matching the pixels from the MAS (or MPIR) with the satellite imagery as noted earlier. The radiance at the top of the atmosphere, that is measured by the satellite, must be estimated from the MPIR (MAS) radiances by computing the impact of the intervening atmosphere on the radiance passing the aircraft level in the direction of the satellite. This will be accomplished through radiative modeling using a variety of techniques including discrete ordinates, adding-doubling, and others. The models will utilize temperature, moisture, aerosol, and ozone data provided by the other instruments.

If only one of the geostationary satellites can be calibrated using the aircraft data because of VZA limitations, the remaining satellites will be intercalibrated to the calibrated sensor by matching FOVs near local noon along the longitude midway between the respective sub-satellite points. If the aircraft data can be used to calibrate more than one of the satellites, then the satellite intercalibrations can serve to estimate the uncertainties in the calibrations.

2) VIS-to-SW conversions

Initially, the narrowband VIS radiances will be converted to SW fluxes using the empirical conversion formulae developed from matched GOES and ERBS scanner data taken over the SGP locale during September and October 1985 and 1986. The GOES radiances are first converted to VIS albedo by applying the proper anisotropic correction factor. The applicable formula and correction factor depend on whether the scene is cloudy or clear. The scene classification is determined using a VIS-IR threshold method

that retrieves cloud amount, height, and optical depth. The derived broadband fluxes will be compared to aircraft-based SW fluxes adjusted to the top of the atmosphere.

In addition to the down-looking BBSW radiometers, lidars, and imagers, uplooking BBSW radiometers should be flown on the UAV or the ER-2. The stratospheric data from task (1) are also needed for this experiment. The UAV and/or the ER-2 should fly a level attitude along flight paths either parallel to the satellite flight path or the scan. The flight patterns should be linear for the narrowband-broadband issue and mapping for the radiance-to-flux problem. The UAV should fly at maximum altitude to minimize the atmospheric correction and to maximize the FOV. The flux radiometers will have a much larger FOV than the MPIR. It is desirable to have the UAV as far from the target as possible to maximize the FOV. However, a full range of scenes needs to be sampled. Thus, there will be conditions (i.e., cirrus) that place the UAV close to the target. Because the ER-2 operates at a nearly constant altitude, The satellite pixels will have to be convolved to match the FOV of the hemispheric sensors. The convolution will include the angular response of the hemispheric sensors and the advection of the cloud field during the interval between the satellite image time and the aircraft pixel time. In most cases, there will be a significant number of pixels matched to each hemispheric FOV.

The flux measurements from the UAV or ER-2 will be adjusted to the top of the atmosphere using radiative transfer calculations and correlated with the matched operational-satellite pixels. The correlations will either be used to examine the error in the empirical narrowband-broadband conversion method or to develop a conversion formula for the SGP and particular satellite. The atmospheric corrections could be tested in two ways that assume good intercalibrations between all of the BBSW radiometers. The first method compares the downwelling fluxes at the UAV level to the measured values to assess the model calculations. The second technique computes the upwelling flux at the ER-2 level using the UAV upwelling fluxes as the lower boundary condition. A comparison of the ER-2 upwelling fluxes to the computed values would yield uncertainty estimates for the atmospheric corrections. A comparison of the relationships derived using only the aircraft instruments and the combined aircraft-satellite data will be used to isolate the anisotropy and convolution errors in the latter method.

Another method for evaluating the flux uncertainties due to the anisotropy of the reflectance fields uses collocated measurements from different satellites. Fluxes can be determined from coincident GOES-8, GOES-9, Meteosat, and AVHRR data at several different times during the day. The differences between the various satellite fluxes will be used to derive the rms. and mean errors in the results. These errors will be due to VIS calibration uncertainties (noted above) and the anisotropic correction factors. The uncertainty due to the angular correction can be separated from the total by assuming it is statistically independent of the VIS calibration uncertainty.

3) SWCRF computations

Shortwave albedos will be computed over the entire SGP domain on a pixel-by-pixel basis for each available satellite image after the calibrations and spectral conversions have been completed. Clear-sky albedo will be also be determined as function of latitude and longitude for each hour over the domain. The satellite data will also be analyzed to retrieve cloud properties which will be related to the SWCRF results. The variability in clear-sky albedo at a given location and local time will be determined from different measurements taken in clear conditions over the course of the experiment. The measurement uncertainties in the both the clear and cloudy sky albedos will be estimated using the differences between the simultaneous, collocated radiances from the array of available satellites and the uncertainties in the narrowband-broadband conversions. The instantaneous total and clear-sky albedos will be averaged over different scales using various weighting factors to correspond to the UAV and/or ER-2 flight paths and the apparent FOVs of the surface instruments. These albedos will be used to compute SWCRF to match the aircraft values. Gridded clear-sky and total albedos will also be integrated for various time periods and scales to ascertain the spatial variability of the derived TOA SWCRF. It is expected that the instantaneous SWCRF values will differ considerably from one satellite to another. Differences between the monthly averages of SWCRF from the various platforms will constitute a overall assessment of the total uncertainty in the TOA SWCRF for a given spatial domain.

A SECOND METHOD FOR DERIVING SHORTWAVE ALBEDOS FROM NARROWBAND SATELLITE MEASUREMENTS

OUTLINE OF THE PROCEDURE

A complementary method for calibrating the satellites will be used to validate the procedure applied in [*Cess et al.*, 1995]. The method is based upon the relationship of narrow and broadband albedos determined directly from instruments on the ER-2. Any procedure for estimating shortwave albedos from narrowband radiances involves three steps:

1. Integration over the upwelling hemisphere;
2. Calibration of the satellite(s) against reference instrument(s); and
3. Conversion from narrow to broadband (unfiltering).

In the present calibration of the GOES satellites, a narrow-band albedo is estimated from the GOES visible channel using the ERBE bi-directional functions (BDRFs) by

$$\alpha_N = \frac{\pi R_N}{\alpha_B(\theta_0,\theta,\phi)}$$

where the terms are defined in table 1.

R_N	Narrow-band reflectance
α_N	Narrow-band Albedo
α_B	Broad-band Albedo
$A_N(\theta_0,\theta,\phi)$	Narrow-band BDRF
$A_B(\theta_0,\theta,\phi)$	ERBE Broadband BDRF
θ_0	Solar Zenith Angle
θ	Sensor Zenith angle
ϕ	Relative azimuth angle Between Sun and sensor

Table 1: Definition of terms

The estimates of α_N are simultaneously calibrated and unfiltered by comparison with coincident measurements of the broadband albedo from the ERBE satellites. The result is an empirical relation between narrow and broad albedos [Cess et al., 1995]:

$$\alpha_B = a_0 + a_1 * \alpha_N + a_2 * \alpha^2_N + a_3 * \ln(\sec \theta_0)$$

The second calibration method will unfilter the narrowband albedos using an empirical relationship determined from the TDDR and solar broadband SBR instruments on the ER-2. The TDDR provides measurements of α_N at 0.5μm, which is very close to the bandpass of the visible channels on the GOES and AVHRR satellites. Estimates of α_N will be derived from satellite measurements R_N and calibrated against the TDDR.

The narrowband albedo at the position and altitude of the ER-2 will be estimated by integrating R_N over the upwelling hemisphere:

$$\alpha_N = 2\int_{\phi=0}^{\pi}\int_{\theta=0}^{\pi/2}\frac{R_N(\vec{x}',\theta_0,\theta',\phi')A_N(\theta_0,\theta,\phi)}{A_N(\theta_0,\theta',\phi')}\cos(\theta)\sin(\theta)d\theta d\phi$$

Here R_N is the satellite radiance for a pixel at a position $\vec{x}$. The origin of the coordinate system is chosen to coincide with the instantaneous ground position of the aircraft. The sun-satellite viewing angles for the pixel at $\vec{x}$ are denoted by θ' and ϕ', and the sun aircraft angles for the same pixel are denoted by θ and ϕ. The radiances emitted from each pixel in the direction of the aircraft are estimated from the radiances measured by the satellite using narrowband BDRFs A_N. These BDRFs will be derived from geostationary and polar satellite measurements over the SGP CART. The rotation of the satellite radiances into the coordinate frame of the aircraft is illustrated in Fig.6.

The satellite albedos will be calibrated against simultaneous measurements from the TDDR. The result will be an empirical relationship.

$$\alpha_N(\text{TDDR}) = f(\alpha_N,...)$$

$$= b_0 + b_1 * \alpha_N + \ldots$$

The conversion from narrow to broadband will be performed by comparing coincident TDDR and SBR albedos:

$$\alpha B(SBR) = g(\alpha_N(TDDR),\ldots)$$
$$= c_0 + c_1 * \alpha_N(TDDR) + \ldots$$

The conversion will be performed for both the 0.3-4.0 μm and 0.3-0.75 μm SBRs. This will permit derivation of the albedos for visible wavelengths where atmospheric absorption is minimal and for the entire shortwave band. The principal advantage of this procedure is that the narrow to broadband conversion is performed using coincident ARESE field measurements from the same platform. In addition, the narrow to broadband conversion is independent of errors in the angular integrations (BDRFs). Systematic errors in the satellite radiometric calibration and the BDRFs only impact the empirical relation between α_N and the TDDR measurements. If necessary, the narrowband BDRFs can be adapted to changes in vegetation and land surfaces (e.g. *Wu et al.*, [1995]). This may be important for ARESE, since there are rapid changes in the ground cover during September and October. The procedure is presently being tested on similar data from the Central Equatorial Pacific Experiment (CEPEX).

SUPPORTING MEASUREMENTS

The radiances measured by the MAS instrument will be used to calibrate the satellite radiances and to correct errors in the satellite telemetry. The MAS data will be used to establish a common normalization between the reflectance's measured by polar and geosynchronous satellites. Since the reflectances depend on the scene type and the sun-satellite viewing geometry (θ_0,θ', and ϕ'), the ER-2 flight tracks will be configured so that a subset of the MAS data has nearly the same viewing geometry as the GOES and AVHRR satellites. The satellite and MAS data will be obtained simultaneously, so the solar zenith angle θ_0 will be identical for both datasets. In order to obtain equivalence

between the sensor zenith angles and relative azimuth angles, the ER-2 will be flown along lines of constant satellite zenith angle θ' (Fig. 7). Since the MAS is a cross-track scanning instrument, this flight plan insures that the lines of constant θ and θ' are parallel. Because the MAS zenith angle θ varies much more rapidly with distance from the ground track of the ER-2 than θ', this flight configuration insures equivalence between θ and θ' for a portion of each MAS so long as $\theta' \leq$ max.(θ). Since the projection of the pixel-to-sensor vector on the Earth's surface is perpendicular to lines of constant θ (or θ') this flight configuration also insures equivalence between ϕ and ϕ'.

For calibration of the AVHRR instruments on the NOAA polar-orbiting satellites, the ER-2 will be aligned with the ground tracks of the satellites. The ground tracks are rotated approximately 8° from the meridional direction, so the ER-2 would fly nearly due north or south for calibration of the AVHRR. The configuration for the calibration of GOES-8 and GOES-9 depends on the position of those satellites at the time of ARESE. GOES-8 is expected to remain at 75W and GOES-9 will be at 90W, although the position of GOES-9 may be changed starting October 19.

The MAS imagery will also be used to correct the navigation of the satellite images. The images from the visible and infrared window channels at 0.66μm and 11μm will be compared to the corresponding images from the satellite scanners. This procedure will minimize the random errors in the calibration procedure introduced by errors in the satellite telemetry.

DATA INTERPRETATION STRATEGIES

The two proposed experiments, the stacked UAV/Otter and the ER2 flying over an array of surface instruments, require different data interpretation strategies. The following describes three strategies for evaluating cloudy-sky atmospheric absorption relative to models, and these apply to both broadband and TDDR measurements. These strategies are demonstrated through use of satellite/surface data sets (Cess et al., 1995) as surrogates for

the respective stacked aircraft and ER2/surface measurements. Naturally, there are other ways to look at the data and alternate analysis is encouraged.

Strategy No. 1.

As discussed by Ramanathan et al. (1995), a direct way of evaluating cloudy-sky SW absorption, relative to that for clear skies, is to compare cloud-radiative forcing (CRF) at the surface to that at the TOA. Atmospheric radiative transfer models typically give

$$CRF(SRF)/CRF(TOA) \approx 1$$

meaning that cloudy skies absorb about the same SW radiation as do clear skies. Recent observations, however, suggest a value for this ratio of about 1.5 (Ramanathan et al., 1995; Cess et al., 1995; Pilewskie and Valero, 1995), indicating that clouds absorb considerably more SW radiation than predicted by models.

Because CRF refers to the difference between all-sky and clear-sky net downward SW radiation, this approach applies to the stacked UAV/Otter measurements, with CRF evaluated at the aircraft altitudes (as in Pilewskie and Valero, 1995) instead of at the TOA and at the surface. Model simulations of CRF are easily performed for the aircraft altitudes.

The collocated GOES and Boulder Atmospheric Observatory (BAO) tower measurements (Cess et al., 1995) serve to illustrate this approach. The GOES/tower measurements are shown in Figs. 8A and 8B as hourly means, although this temporal averaging need not apply to the aircraft measurements. Evaluation of CRF(SRF) and CRF(TOA) requires identification of clear-sky measurements which, for a given solar zenith angle, correspond to the maximum values of net downward SW at both the TOA and at the surface. These are represented by linear fits in Fig. 8. The difference between each measurement and the clear-sky fit provides CRF for each measurement. Because theoretical models typically yield $CRF(SRF)/CRF(TOA) \approx 1$, the observed value of 1.46 means the cloudy atmosphere is absorbing roughly 30 W m^{-2} (dayside mean) more SW radiation than expected, this being the difference between CRF(TOA) and CRF(SRF).

Strategy No. 2.

While the preceding has the advantage of directly appraising the enhanced cloudy-sky absorption (30 W m^{-2} dayside mean), the ER2/surface measurements will not provide net surface SW, but instead surface insolation. Nevertheless this still allows an appraisal of cloudy-sky absorption by defining a cloud surface forcing in terms of surface insolation rather than net surface SW. This is demonstrated in Fig 8C, for which CIF(SRF)/CRF(TOA) = 1.75, in contrast to 1.25 for models that produce CRF(SRF)/CRF(TOA) ≈ 1. Thus the 1.75 (Fig. 8C) versus 1.25 conveys the same message as 1.46 (Fig. 8B) versus 1.0; observed clouds absorb more SW radiation than do model clouds.

For the American Samoa data, CRF(TOA) from Fig. 9A, together the CIF(SRF) from Fig. 9B, again demonstrate that, when compared to version 2 of the NCAR Community Climate Model (CCM2), that models underestimate cloud SW absorption (Fig. 10), as also applies to the Cape Grim data.

Strategy No. 3

Yet an alternate approach is to note that

$$CIF(SRF)/CRF(TOA) = -(I - I_c)/S(\alpha - \alpha_c)$$

where I is the surface insolation, S is the TOA insolation, α is the TOA albedo, and the subscript c refers to clear skies. With T = I/S being the atmospheric transmittance, the above may be rephrased as

$$CIF(SRF) / CRF(TOA) = -(\Delta\alpha/\Delta T)^{-1}$$

where Δ denotes the all-sky minus clear-sky difference. The alternate approach is to evaluate $\Delta\alpha/\Delta T$ from a linear regression; the advantage is that this does not require clear sky identification. Figure 9 demonstrates, for American Samoa, Boulder and Cape Grim, that the two approaches yield consistent results.

DATA ANALYSIS SUMMARY

Strategies Numbers 1 and 2 are applicable, respectively, to the stacked UAV/Otter and ER2/surface experiments, except that the hourly-mean constraint in the satellite/surface measurements will not be a constraint to this program. Some sort of averaging, however, may be useful for the purpose of reducing sampling errors. Due to the possibility of broken cloud effects, it is imperative that strategy Number 3 be used in all cases, as this serves to remove cloud SW absorption from broken cloud effects.

INTENSIVE FIELD OPERATIONS

OPERATIONS PLANS

The ARESE Project Office and the ARESE science team (AST) will prepare detailed operations plans for the observational component of ARESE. These plans must be developed as soon as possible in light of the short lead time and must follow the guidelines established in this document. The individuals responsible for the surface and aircraft operations must work in coordination with the project manager and the chief scientist in the development of operational plans

CHIEF PROJECT SCIENTIST AND PROJECT MANAGER

Dr. Francisco P. J. Valero has been appointed as the ARESE Chief Project Scientist, Dr. Stephen E. Schwartz has been appointed as the Project Manager. They will coordinate the planning and implementation of the science objectives, conduct planning and debriefing sessions.

The chief scientist will be the scientific spokesperson for the overall field experiment and be the chief representative of and arbitrator for the participants in the field mission.

ARESE SCIENCE TEAM

The following scientists have been designated members of the ARESE Science Team, based on their scientific qualifications, interest in the project, participation in the design of the project and expected participation during the project and in the interpretation of the scientific results:

T. Ackerman, Penn State
R. Cess, Stony Brook
W. Collins, Scripps
R. Ellingson, Maryland
C. Gautier, Santa Barbara
J. Kiehl, NCAR
K. N. Liou, Utah
P. Minnis, NASA Langley
P. Pilewskie, NASA Ames
V. Ramanathan, Scripps
S. Schwartz, Brookhaven
G. Stokes, Battelle Northwest
T. Tooman, Sandia
F. P. J. Valero, Scripps
J. Vitko, Sandia
C. Whitlock, NASA Langley
B. Wielicki, NASA Langley
W. Wiscombe, NASA Goddard
M-H Zhang, Stony Brook

MISSION SELECTION TEAM

During the intensive field phase of the ARESE activities, a Mission Selection Team (MST) will be formed. The MST will be comprised of no more than five AST scientists and the Chief Project Coordinator. It will be chaired by the AST Chief Scientist. The MST will accept the following responsibilities:

i. solicit and represent ideas of other ARESE scientists in operations, decisions, and scheduling

ii. review on a daily basis the candidate missions proposed by the MPT (see section below) and select the planned operations and scheduling of all ARESE platforms for the following day.

iii. select on a daily basis a Mission Scientist (MS) and an Alternate Mission Scientist to plan and carry out operations selected by the MST.

iv. assemble forecast information for use in daily operations planning.

v. maintain up-to-date experiment accomplishment records for use in daily operations planning.*

vi. maintain current status reports on all data gathering components throughout the experiment.*

vii. review daily post mission reports prepared by the Mission Planning Team (see section below).

*assisted by the ARESE Project Office.

All deliberations of the Mission Selection Team will be open and in the absence of a clear consensus among its members, the chairman will assume responsibility for making operations decisions.

On issues concerning specific platforms such as aircraft or special sonde ascents, an appropriate spokesperson from the contributing organization will be given the opportunity to advise the MST and to participate on the MPT.

MISSION PLANNING TEAM

A Mission Planning Team (MPT) will be active during the field observations period. The Mission Planning Team will contain at least three AST members, individuals representing participating aircraft facilities, each platform mission scientist and ARESE Project Office support personnel. The MPT members for the following day will be identified on a daily basis by the MST. Ideally, on any given day, the MPT will contain candidate mission scientists for the following day's operations. It will not be uncommon for members of the MST to also serve as members of the MPT. The MPT's responsibilities are listed below.

i. Prepare candidate missions for the following day's operations and present these to the MST for consideration.

ii. Following a decision by the MST, support the Mission Scientist in preparing a detailed mission plan for the following day's operations.

iii. Prepare a post mission summary of each day's operations including an evaluation of the success of the operations. This daily summary will be made available to the ARESE Project Office and the MST and become a part of the ARESE data archives

MISSION SCIENTIST

A Mission Scientist (MS) and an alternate MS will be identified on a daily basis by the MST at the same time the following day's mission is selected. The MS will be in charge of the detailed planning of the following day's operations and the execution of that plan. He will be responsible for making any real time decision required during the execution of the plan. He will oversee the preparation of a post mission summary of each day's operations including an evaluation of the success of the operations.

A Mission Scientist must have an overall grasp of the scientific objectives of ARESE as well as an appreciation of operational constraints of the various platforms and personnel.

The Mission Scientist will be selected from the AST researchers according to the scientific objectives to be addressed in the upcoming mission and the scientific background of the individual. Ideally, the Mission Scientist would be the previous mission's Alternate Mission Scientist so as to provide continuity between missions and familiarity with on-going meteorology conditions and forecasts.

IFO MISSION AND DATA SCHEDULE

SIMULATED IFO

Approximately 2-3 months before the intensive field mission, a simulated IFO will be conducted at an appropriate site. The purpose of the meeting will be to simulate the mission planning, based on realistic meteorological conditions and using those major platform instruments that will participate in the actual IFO. Representatives from the satellite, aircraft, and surface-based instruments will participate, as well as the IFO meteorologist/forecaster) and other key researchers.

Meteorology forecasts will be based on actual meteorology conditions experienced by the IFO area one year previously.

The mission planning will include: research objectives to be addressed; platforms/instruments that will operate; and deployment strategy including flight plans, operating schedules, data taking modes, etc. Constraints to be considered include finite resources (aircraft flight hours allocated, cost of sonde/satellite data, etc.), realistic operational schedules (aircraft/crew constraints, personnel/instrument fatigue, etc.), uncertainty of meteorology forecast, etc. The mission plans will be evaluated for expected results, based on actual meteorological conditions experienced on the mission day, and improvements/modifications will be discussed. The meteorological forecast for the next day will be presented and the cycle repeated.

PRE-MISSION MEETING

A pre-mission meeting will be held on the day before the start of the intensive field mission. The purpose of the meeting will be to welcome all participants, describe the mission operations strategy, provide information on local logistics, determine the operational status of the participating platforms/instruments, and allow the local media an opportunity to interact with the mission, principal investigators, and other participants. A mission planning meeting for the first day of operations will follow immediately.

POST FLIGHT DEBRIEF

After each experiment flight there will be a post-flight debriefing with all the experimenters. This debriefing is intended to communicate and document pertinent subjective observations made during the completed mission and allow the experimenters an opportunity to modify subsequent plans or procedures for the following experiment. Each experimenter should have a "quick-look" capability for inspection of their sensor performance. A copy of the "quick-look" data (raw strip charts, tables, etc.) may be submitted to the Data Manager for possible comparison/correlation with other experiment data.

POST-MISSION DEBRIEF

A post-mission debriefing will be held on the day following the conclusion of the mission. Each experimenter will describe their sensor performance, a summary of sensor operating times, a sample of data obtained, a description of the data format that is planned to be submitted to the data archives and a listing of experiment days to be analyzed in a priority order. The Working Group will review the missions and measurements obtained during the mission. If appropriate, it will prioritize experiment days to be analyzed, key areas of data reduction and analysis, identify possible data collaboration and exchange.

DATA PROTOCOL AND PUBLICATION PLAN

The ARESE data protocol has been prepared to encourage the timely data release, analysis and publication of scientific results. The ARESE data from all platforms will be made available for archiving within three months from the date of the last field experiment activity.

The ARESE science team is responsible for the certification of the data submitted to the permanent data archive. This certification is one of the objectives of the Data Workshop (see below).

REFERENCES

1. G. L. Stephens and S. Tsay, *Q. J. R. Meteorol. Soc.* **116**, 671 (1990).
2. R. D. Cess et al., *Science 267*, 496 (1995).
3. V. Ramanathan, et al., *Science 267*, 499 (1995).
4. P. Pilewskie and F. P. J. Valero, *Science, 267*, (1995).
5. F. P. J. Valero et al., *Geophys. Res. Lett.* **10**, 1184 (1983); F. P. J. Valero et al., *Geophys. Res. Lett.* **11**, 465(1984)
6. Z. Q. Li et al., *J. Clim.* **6**, 317 (1993)
7. Wu, A., Li, and J. Cihlar, *J. Geophys. Res., 100*, 9179-9192, 1995.
8. Rao, C.R.N., J. Chen, F.W. Staylor, P. Abel, Y.J. Kaufman, E. Vermote, W.R. Rossow and C. Brest. *Technical Report NOAA NESDIS 70, National Oceanographic and Atmospheric Administration*, 1993.
9. Suttles, J.T., *NASA Ref. Publ.* 1184, 1988.

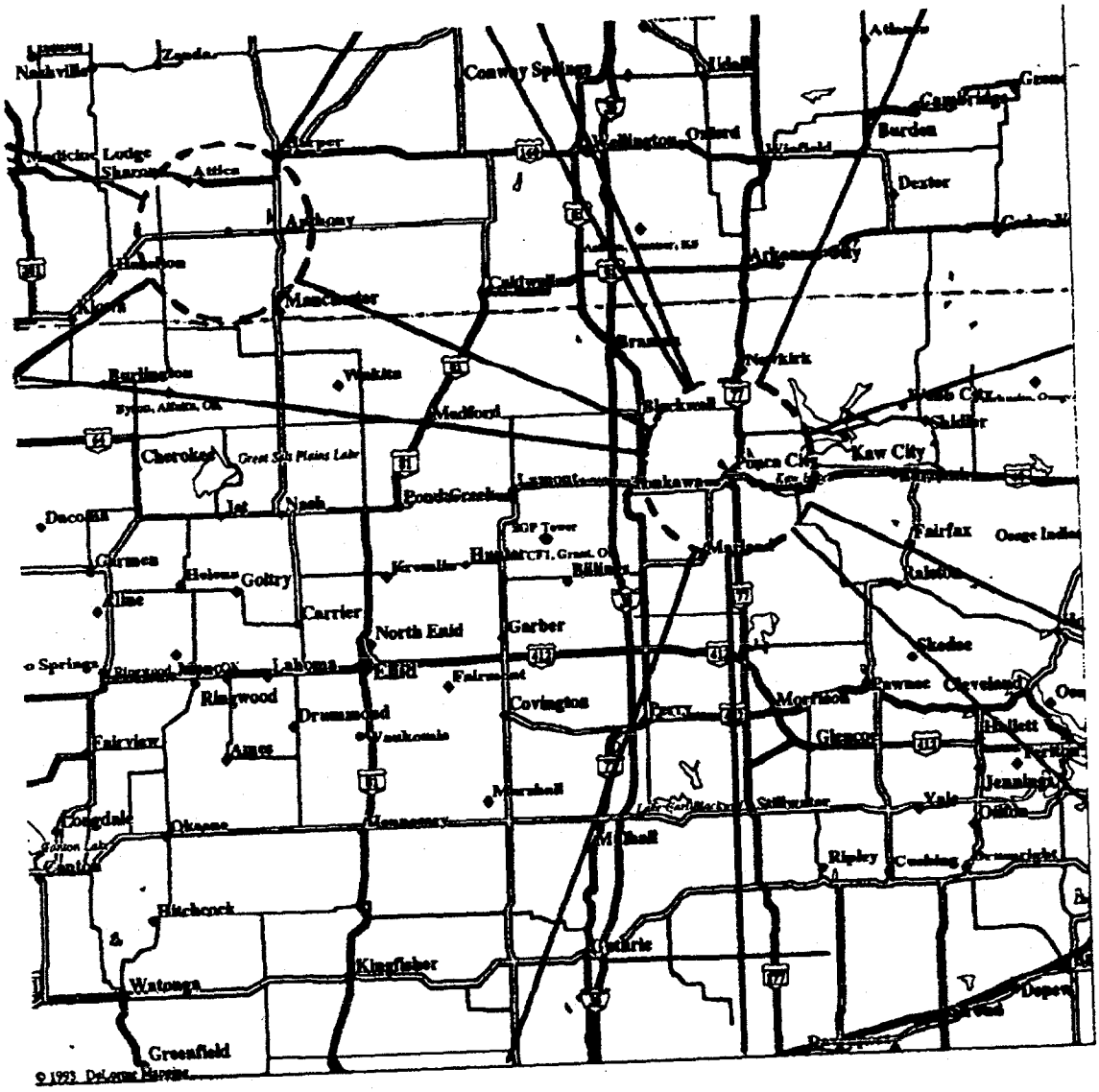

LEGEND

- Town, Small City
- Large City
- Interstate, Turnpike
- US Highway
- State/Prov Boundary
- Population Center
- Major Street/Road
- Interstate Highway
- State Route
- US Highway
- Open Water

Scale 1:1,000,000 (at center)

20 Miles

20 KM

Mag 9.00

Tue Jun 03 15:26:54 1995

ARESE Flight Track B

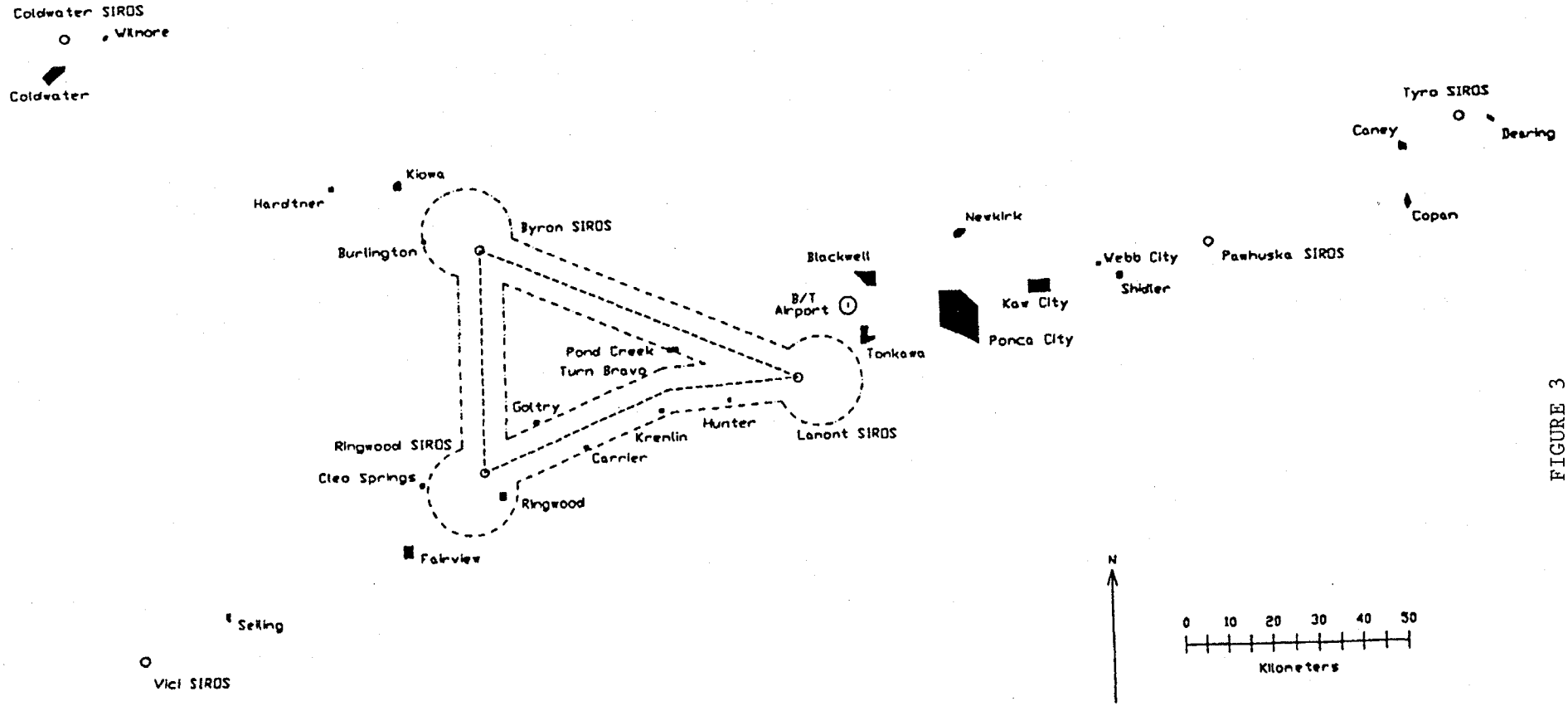

FIGURE 3

ARESE Flight Track C

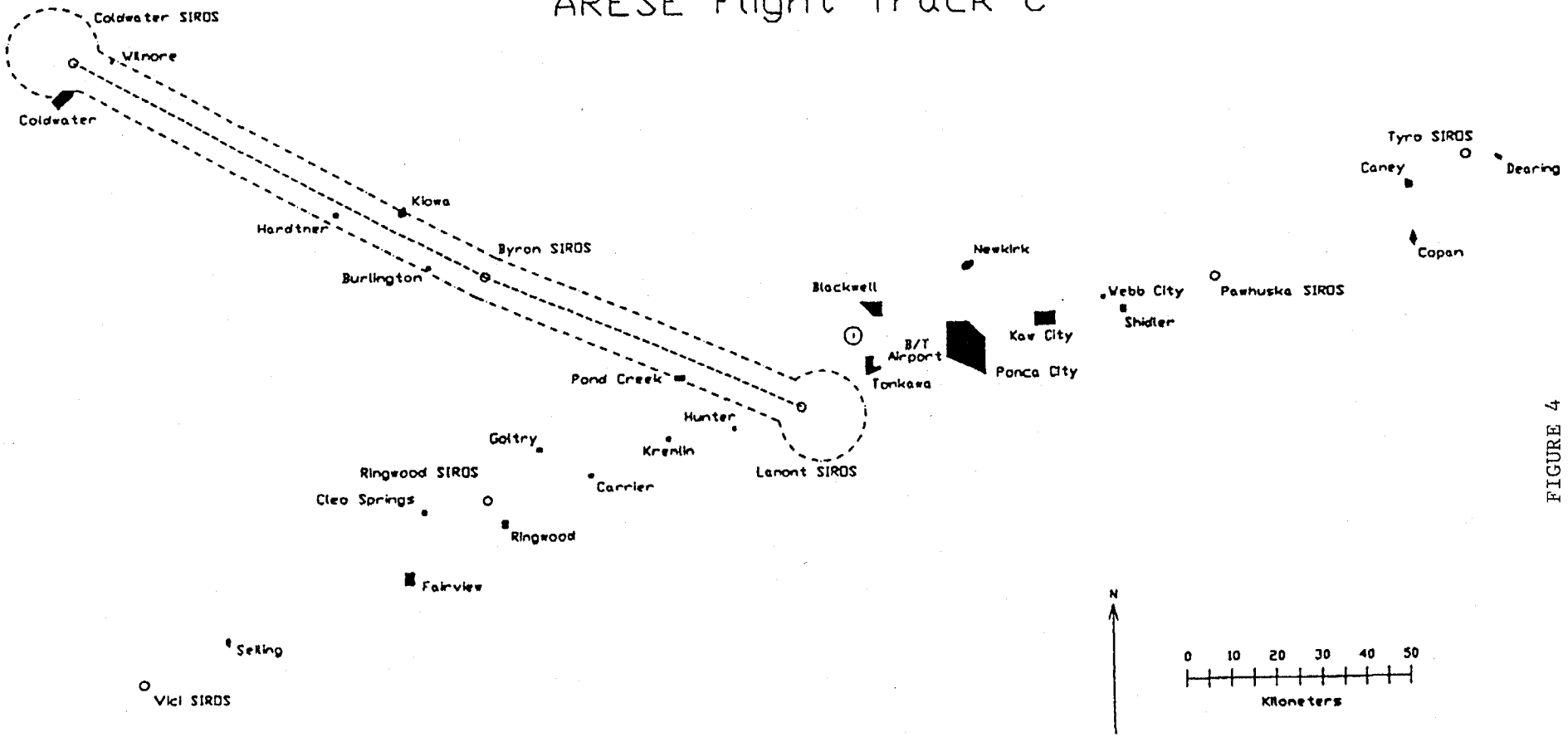

FIGURE 4

ARESE Flight Track D

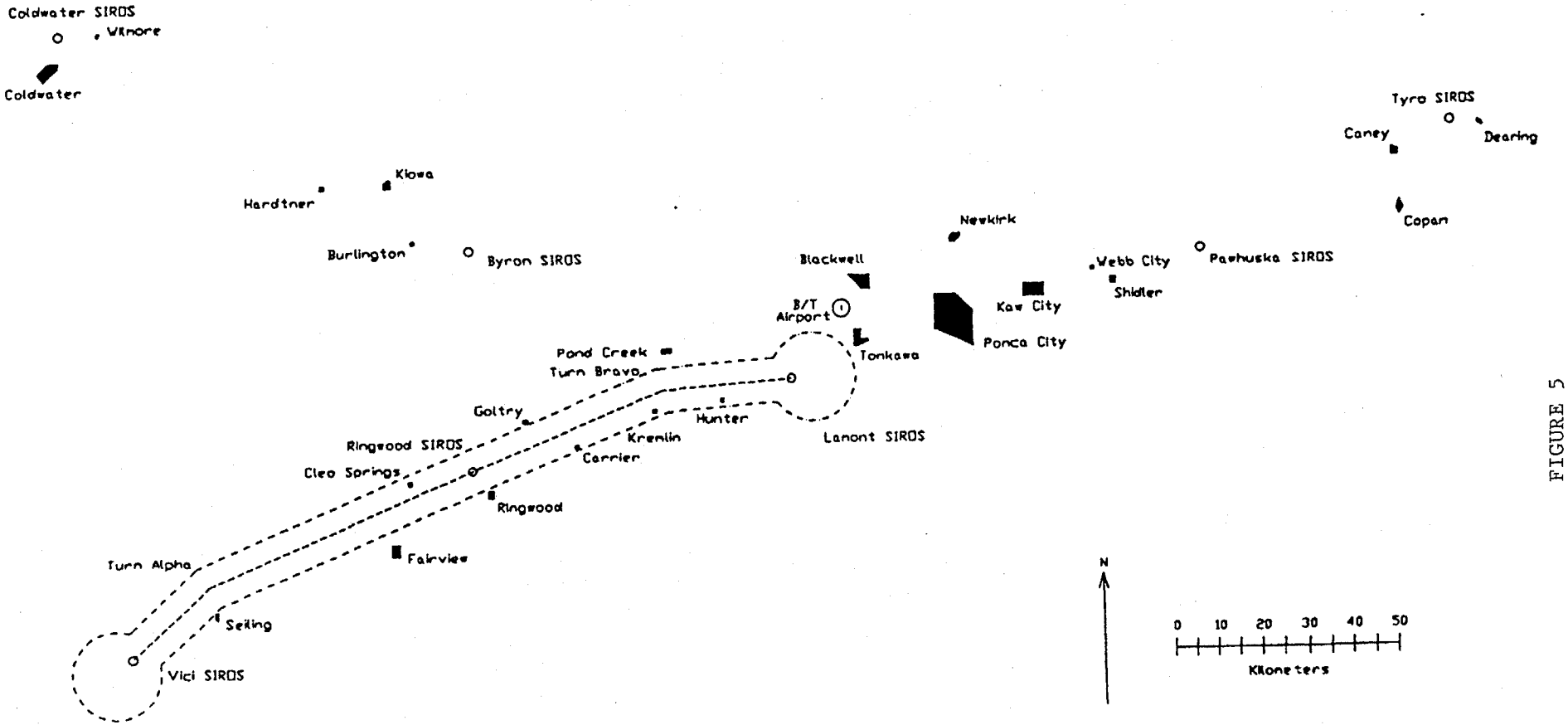

FIGURE 5

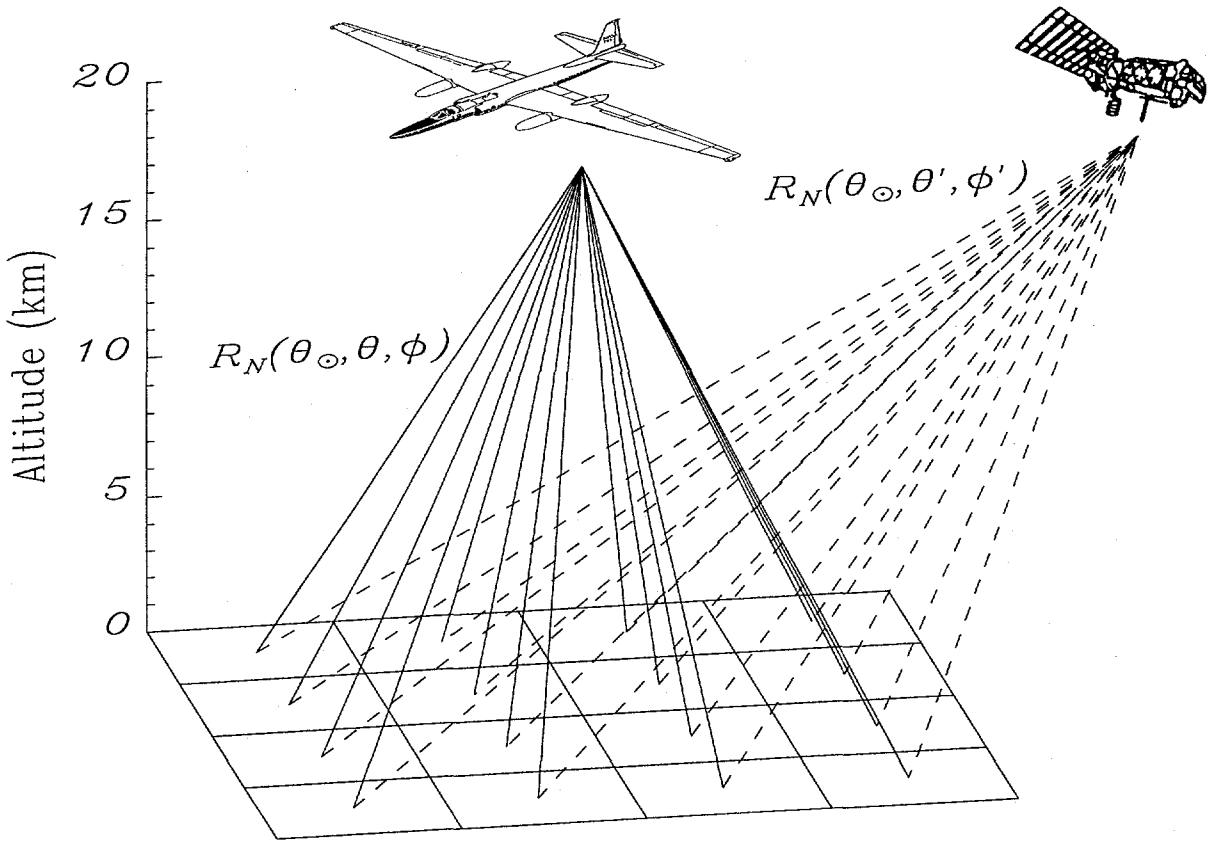

Figure 6: Schematic of hemisphere integration of upwelling narrowband radiances in the aircraft coordinate frame

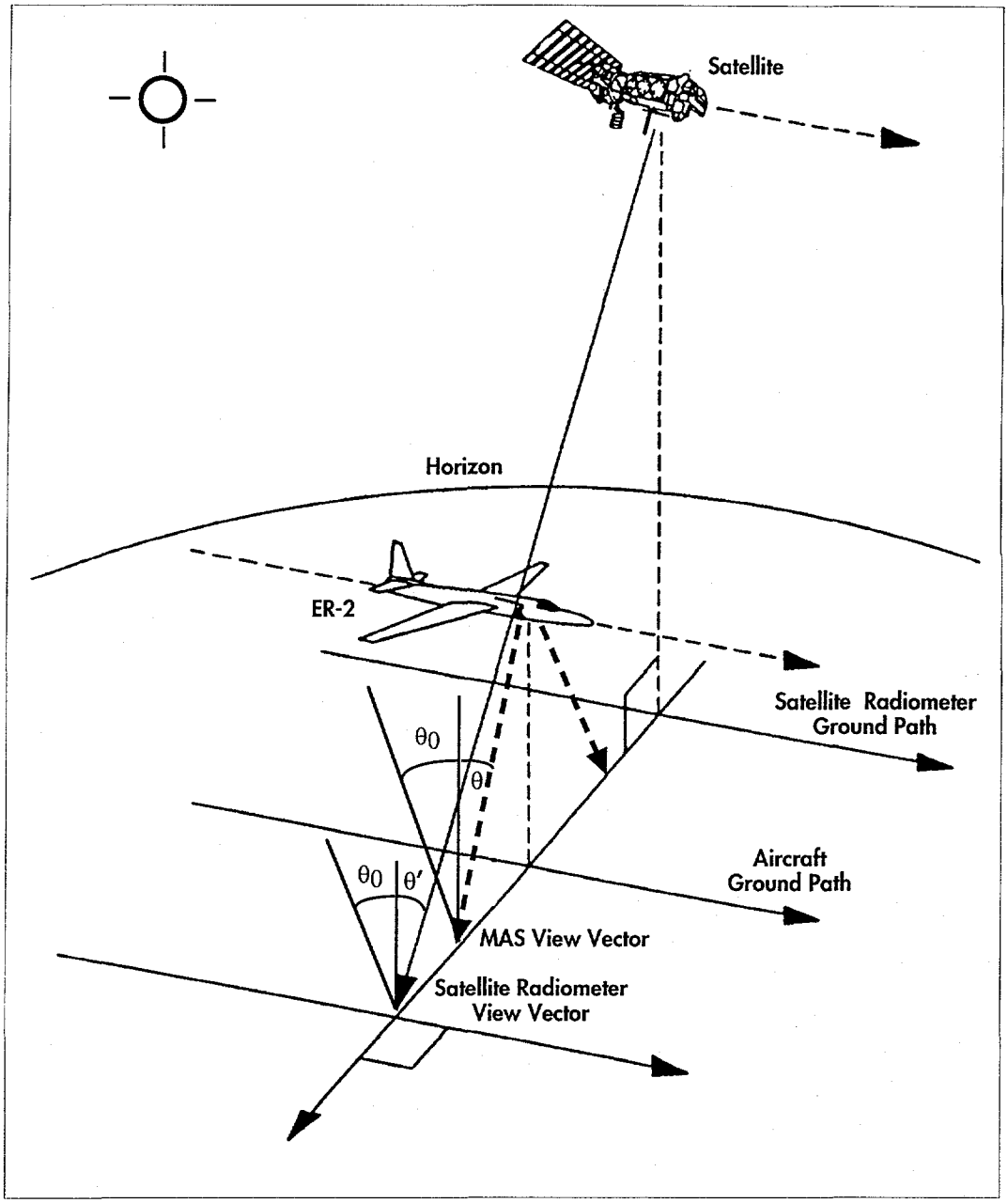

Figure 7: Flight plan for ER-2 for intercalibration between the MAS and satellite radiometers (after Rao et al. [1993]).

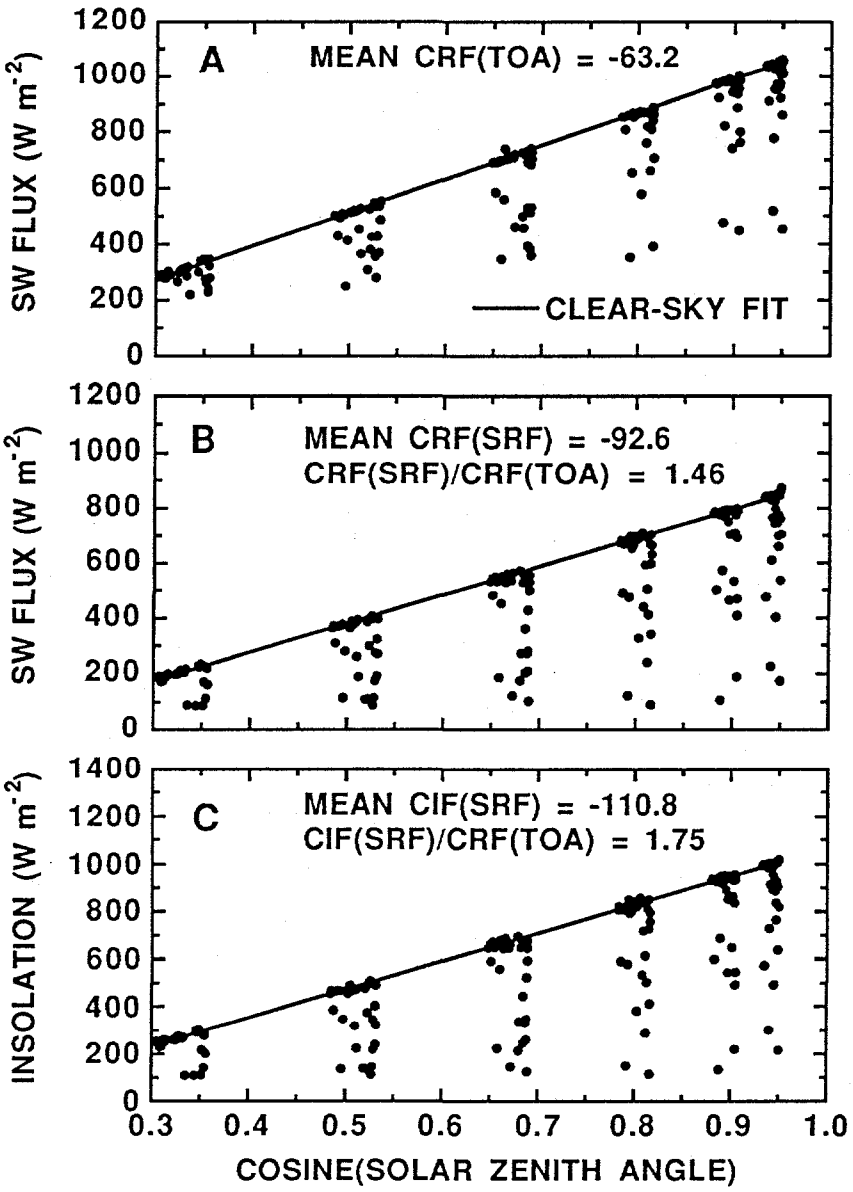

Fig. 6. (A) The net downward SW flux at the TOA, as measured by GOES at the BAO tower, as a function of the cosine of the solar zenith angle. (B) The same as (A) but for the tower-measured net downward SW flux at the surface. (C) The same as (A) but for the tower-measured surface insolation.

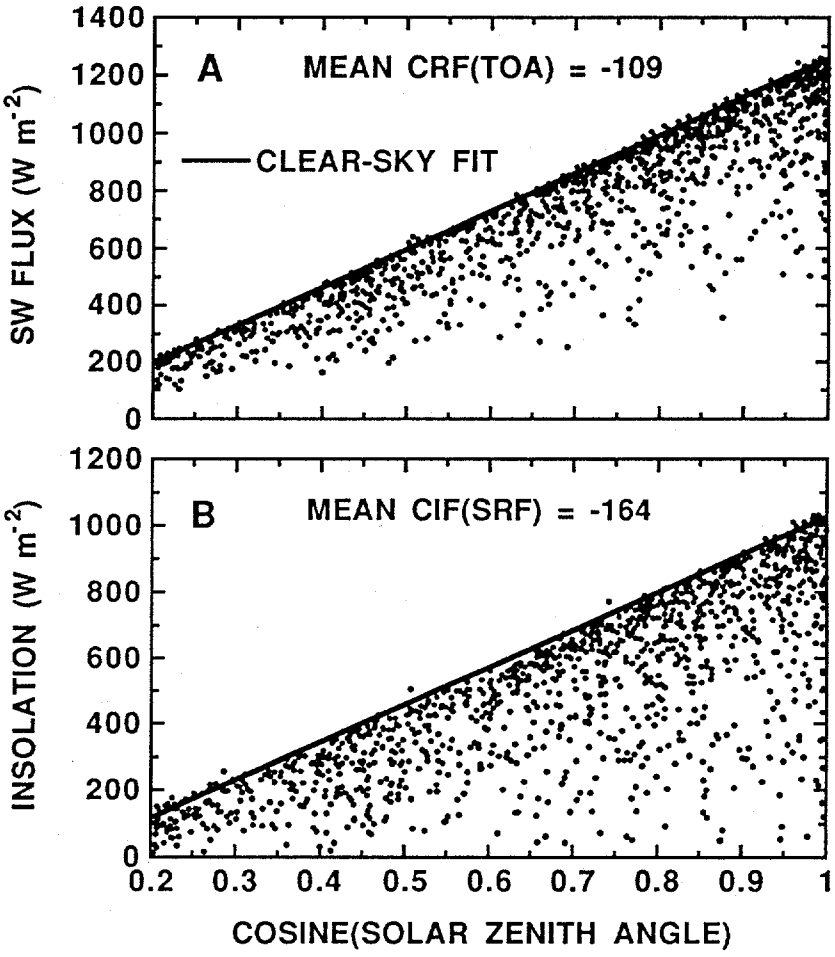

Fig. 1. (A) The net downward SW flux at the TOA, as measured by ERBS at American Samoa, as a function of the cosine of the solar zenith angle. (B) The same as (A) but for the surface insolation.

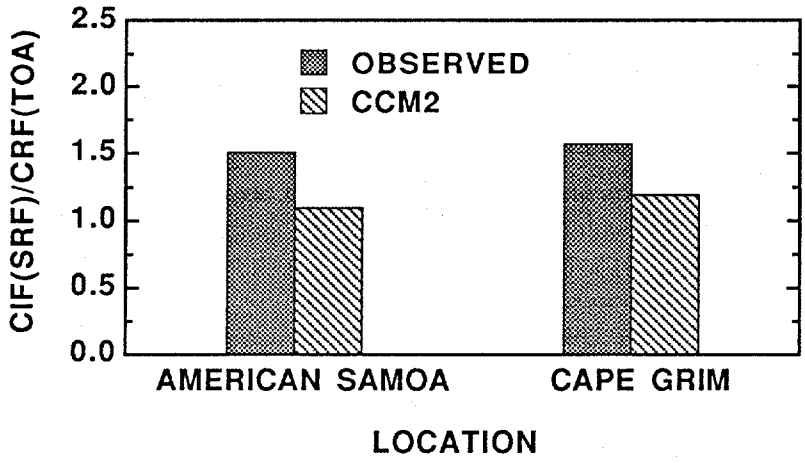

10
Fig. 8. Comparison of CIF(SRF)/CRF(TOA) determined from CCM2 to the observed values for American Samoa and Cape Grim.

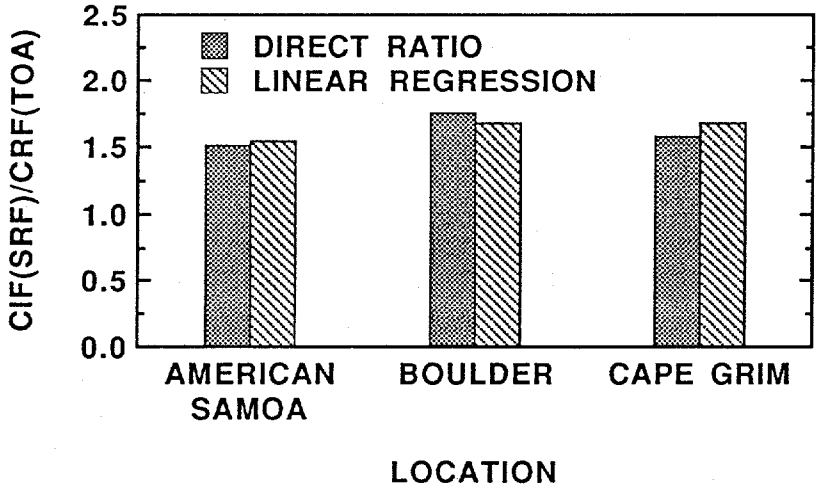

11
Fig. 9. Comparison of CIF(SRF)/CRF(TOA) determined directly and from a linear regression.

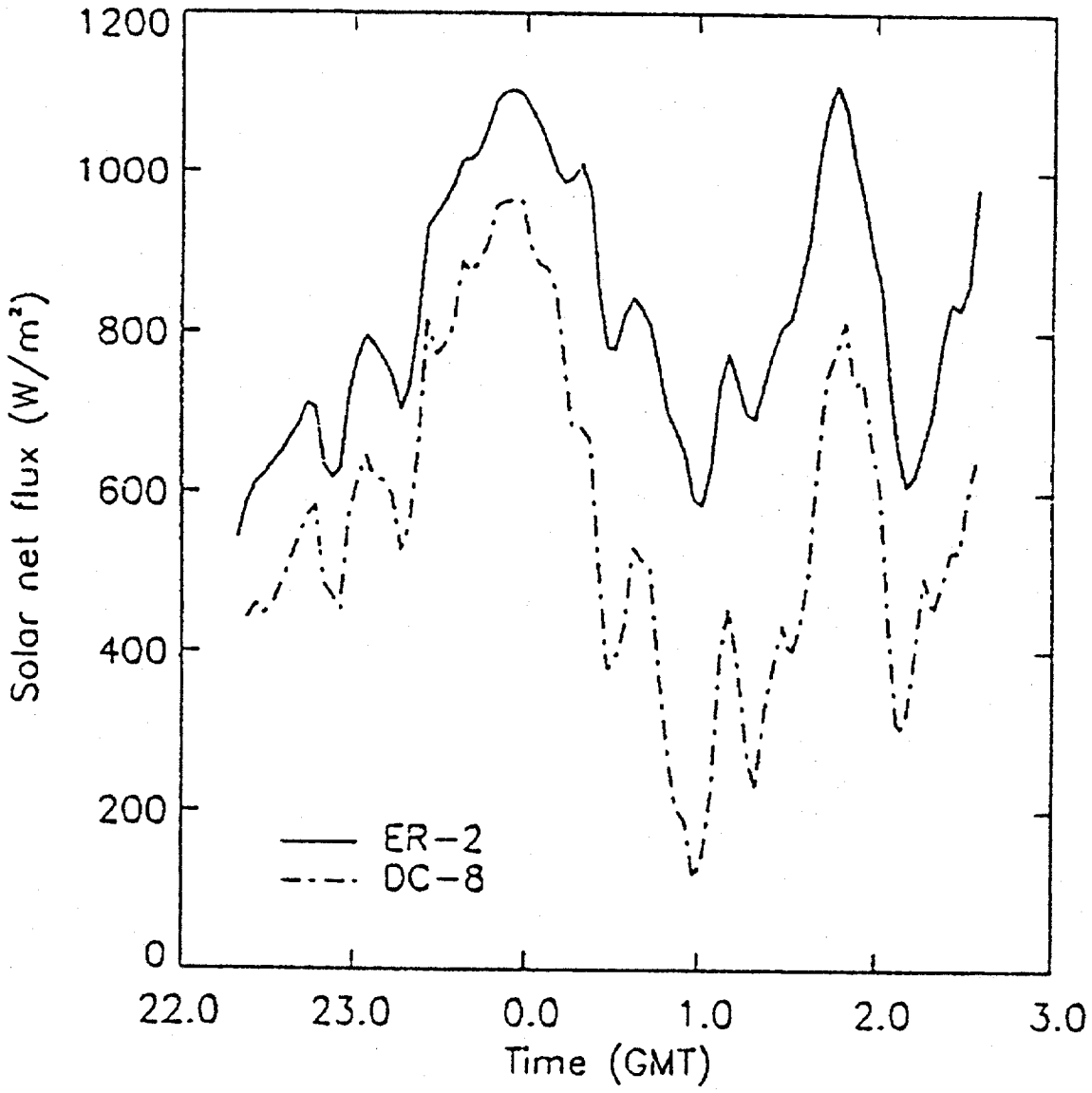

FIGURE 1. (Source Pilewskie and Valero Science 267, 1626, 1995). Example of net solar fluxes measured simultaneously from the ER-2 and DC-8 during coordinated flight.